

System-dependent exchange–correlation functional with exact asymptotic potential and $\epsilon_{\text{HOMO}} \approx -I$

Jonathan D. Gledhill and David J. Tozer

Citation: *The Journal of Chemical Physics* **143**, 024104 (2015); doi: 10.1063/1.4926397

View online: <http://dx.doi.org/10.1063/1.4926397>

View Table of Contents: <http://scitation.aip.org/content/aip/journal/jcp/143/2?ver=pdfcov>

Published by the [AIP Publishing](#)

Articles you may be interested in

[Generalized gradient approximation exchange energy functional with correct asymptotic behavior of the corresponding potential](#)

J. Chem. Phys. **142**, 054105 (2015); 10.1063/1.4906606

[Correlation energy functional and potential from time-dependent exact-exchange theory](#)

J. Chem. Phys. **132**, 044101 (2010); 10.1063/1.3290947

[A semiempirical generalized gradient approximation exchange–correlation functional](#)

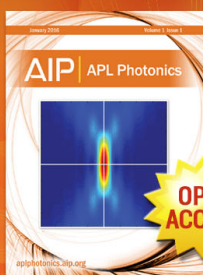
J. Chem. Phys. **121**, 5654 (2004); 10.1063/1.1784777

[Assessment of exchange–correlation functionals for the calculation of dynamical properties of small clusters in time-dependent density functional theory](#)

J. Chem. Phys. **115**, 3006 (2001); 10.1063/1.1385368

[Kohn–Sham calculations using hybrid exchange–correlation functionals with asymptotically corrected potentials](#)

J. Chem. Phys. **113**, 5185 (2000); 10.1063/1.1290002



Launching in 2016!
The future of applied photonics research is here

OPEN
ACCESS

AIP | APL
Photonics

System-dependent exchange–correlation functional with exact asymptotic potential and $\epsilon_{\text{HOMO}} \approx -I$

Jonathan D. Gledhill and David J. Tozer^{a)}*Department of Chemistry, Durham University, South Road, Durham DH1 3LE, United Kingdom*

(Received 13 May 2015; accepted 25 June 2015; published online 9 July 2015)

Density scaling considerations are used to derive an exchange–correlation explicit density functional that is appropriate for the electron deficient side of the integer and which recovers the exact $r \rightarrow \infty$ asymptotic behaviour of the exchange–correlation potential. The functional has an unconventional mathematical form with parameters that are system-dependent; the parameters for an N -electron system are determined in advance from generalised gradient approximation (GGA) calculations on the N - and $(N - 1)$ -electron systems. Compared to GGA results, the functional yields similar exchange–correlation energies, but HOMO energies that are an order of magnitude closer to the negative of the vertical ionisation potential; for anions, the HOMO energies are negative, as required. Rydberg excitation energies are also notably improved and the exchange–correlation potential is visibly lowered towards the near-exact potential. Further development is required to improve valence excitations, static isotropic polarisabilities, and the shape of the potential in non-asymptotic regions. The functional is fundamentally different to conventional approximations. © 2015 AIP Publishing LLC. [<http://dx.doi.org/10.1063/1.4926397>]

I. INTRODUCTION

A plot of the exact electronic energy as a function of electron number comprises a series of straight line segments, with derivative discontinuities at the integers.¹ Kohn–Sham density functional theory (DFT) calculations² using approximate exchange–correlation functionals fail to reproduce this piecewise linearity. This failure—termed delocalisation error^{3–5} or many-electron self-interaction error^{6–11}—leads to errors in a wide range of computed quantities.^{3,4,12–16}

One way to try to reduce these errors is to demand that the exchange–correlation functional approximately reproduces conditions associated with the exact piecewise linearity. For explicit density functionals and orbital-dependent functionals within the usual generalised Kohn–Sham (GKS) formalism,¹⁷ the slopes of the calculated energy vs. electron number curve on the electron deficient and electron abundant sides of an integer are equal to the calculated HOMO and LUMO energies of the integer system, ϵ_{HOMO} and ϵ_{LUMO} , respectively.¹³ Note that the terminology “electron deficient/abundant” refers to the limiting behaviour as the electron number approaches integer from below/above. The corresponding slopes of the exact piecewise linear curve are the negative of the exact vertical ionisation potential I^0 and electron affinity A^0 of the integer system, respectively, and so it is desirable to satisfy the Koopmans conditions,

$$\epsilon_{\text{HOMO}} = -I^0, \quad (1)$$

$$\epsilon_{\text{LUMO}} = -A^0. \quad (2)$$

These conditions have been widely and successfully used^{18–35} to “tune” orbital-dependent, global and range-separated hybrid functionals within the GKS formalism. The

HOMO and LUMO energies vary systematically with the parameter defining the amount of (long-range) exact orbital exchange and so this parameter is varied on a system-by-system basis in order to approximately satisfy one or both of the conditions. Of course, exact ionisation potentials and electron affinities are not generally available and so these are usually replaced with approximate values calculated from DFT total electronic energies. See Ref. 30 for a recent assessment of such tuning approaches.

For explicit density functionals, such as local functionals or generalised gradient approximations (GGAs), the situation is less straightforward. The lack of exact orbital exchange means that there is no obvious parameter that can be varied to adjust the HOMO and LUMO energies in a systematic manner. Furthermore, unlike in global/range-separated hybrid GKS calculations, where the non-multiplicative nature of the exchange–correlation operator means Eqs. (1) and (2) can both be approximately satisfied at the same time, the exchange–correlation potential is now multiplicative and it is not in general possible to satisfy both conditions. This can be traced to the fact that the piecewise linearity of the exact energy leads to a jump in the exact exchange–correlation potential (by an amount Δ_{xc} , which is typically several electron volts) as the electron number increases through an integer; this is the so-called integer discontinuity.¹ The exact potential on the electron deficient side of the integer does yield a HOMO energy that satisfies Eq. (1); however it is the *shifted* potential on the electron abundant side of the integer that yields a LUMO energy that satisfies Eq. (2). Local functionals and GGAs are continuum approximations, meaning they exhibit a potential that is continuous across the integer, so there is only one potential for the integer system, which cannot satisfy both conditions. In fact, these functionals yield a potential that approximately averages over the discontinuity, meaning

^{a)}Electronic mail: d.j.tozer@durham.ac.uk

HOMO energies are well above $-I^0$ and LUMO energies are well below $-A^0$ (Ref. 36).

In the present study, we propose a method for deriving an exchange–correlation explicit density functional for a system with integer electron number N , which does approximately satisfy one of the Koopmans conditions. Specifically, we choose Eq. (1), and so it amounts to a method for deriving a functional that is appropriate for the electron deficient side of the integer. Our approach is based on density scaling and so we commence by outlining the key aspects of density scaling, paying particular attention to the influence of the integer discontinuity. We then go on to derive, analyse, and assess the performance of a functional. Future research directions are then outlined and conclusions are drawn.

II. METHODOLOGY AND RESULTS

A. Density scaling and influence of the integer discontinuity

A functional $F[\rho]$ is homogeneous of degree k under density scaling if it satisfies

$$F[\xi\rho] = \xi^k F[\rho] \quad (3)$$

or equivalently (for $k \neq 0$),³⁷

$$k = \frac{\int v_F(\mathbf{r})\rho(\mathbf{r}) d\mathbf{r}}{F[\rho]}, \quad (4)$$

where $v_F(\mathbf{r}) = \delta F[\rho]/\delta\rho(\mathbf{r})$ and $\rho(\mathbf{r})$ is the electron density. The evaluation of the quantity k in Eq. (4) therefore provides a simple mechanism for quantifying the behaviour of any functional $F[\rho]$ under density scaling. If the value of k is system-independent, then the functional is homogeneous of degree k . If the value of k is system-dependent, then the functional is inhomogeneous and the degree of system-dependence provides a measure of the degree of inhomogeneity.

In a recent study,³⁸ we used Eq. (4) to study the density scaling properties of the exchange–correlation functional. Following Zhao, Morrison, and Parr,³⁹ we defined a system-dependent “effective homogeneity”

$$k_{xc} = \frac{\int v_{xc}(\mathbf{r})\rho(\mathbf{r}) d\mathbf{r}}{E_{xc}[\rho]}, \quad (5)$$

where $E_{xc}[\rho]$ is the exchange–correlation energy functional and $v_{xc}(\mathbf{r}) = \delta E_{xc}[\rho]/\delta\rho(\mathbf{r})$ is the exchange–correlation potential. We then evaluated this quantity for atoms and molecules at equilibrium geometries using near-exact exchange–correlation potentials, electron densities, and exchange–correlation energies, determined from experimental and correlated *ab initio* data. A key aspect of the study was the influence of the integer discontinuity in the exact exchange–correlation potential. On the electron deficient side of the integer, the exact potential decays to zero as $-1/r$ and yields the HOMO energy in Eq. (1); we denote this potential $v_{xc}^-(\mathbf{r})$. On the electron abundant side, the exact potential is shifted from $v_{xc}^-(\mathbf{r})$ at all points in space by the integer discontinuity Δ_{xc} and yields the LUMO energy in Eq. (2); we denote this potential

$$v_{xc}^+(\mathbf{r}) = v_{xc}^-(\mathbf{r}) + \Delta_{xc}. \quad (6)$$

We evaluated k_{xc} using our best estimates for $v_{xc}^-(\mathbf{r})$, $v_{xc}^+(\mathbf{r})$, and the average of two, denoted $v_{xc}^{av}(\mathbf{r})$, to give three near-exact effective homogeneities,

$$k_{xc}^- = \frac{\int v_{xc}^-(\mathbf{r})\rho(\mathbf{r}) d\mathbf{r}}{E_{xc}[\rho]}, \quad (7)$$

$$k_{xc}^+ = \frac{\int v_{xc}^+(\mathbf{r})\rho(\mathbf{r}) d\mathbf{r}}{E_{xc}[\rho]} = k_{xc}^- + \frac{N\Delta_{xc}}{E_{xc}[\rho]}, \quad (8)$$

and

$$k_{xc}^{av} = \frac{\int v_{xc}^{av}(\mathbf{r})\rho(\mathbf{r}) d\mathbf{r}}{E_{xc}[\rho]} = k_{xc}^- + \frac{N\Delta_{xc}}{2E_{xc}[\rho]}. \quad (9)$$

Both k_{xc}^- and k_{xc}^+ are relatively system dependent, whereas k_{xc}^{av} is close to 4/3. See Ref. 38 for full details.

The quantities k_{xc}^- are the effective homogeneities for a functional that is appropriate for the electron deficient side of the integer, i.e., for a functional that essentially (a) yields the exact E_{xc} , (b) yields the exact electron deficient potential $v_{xc}^-(\mathbf{r})$, and (c) yields a HOMO energy that satisfies Eq. (1). The central idea of the current study is that *we can determine a functional appropriate for the electron deficient side of the integer by demanding that it yields effective homogeneities, k_{xc} in Eq. (5), that are close to k_{xc}^- .*

In addition to density scaling, it is pertinent to comment on the more common concept of coordinate scaling.⁴⁰ A functional $F[\rho]$ is homogeneous of degree m under coordinate scaling if

$$F[\rho_\lambda] = \lambda^m F[\rho], \quad (10)$$

where the coordinate-scaled density is

$$\rho_\lambda(\mathbf{r}) = \lambda^3 \rho(\lambda\mathbf{r}). \quad (11)$$

B. Functional derivation and implementation

We require a functional that yields effective homogeneities that are close to k_{xc}^- . One way forward would be to express $E_{xc}[\rho]$ as a linear combination of system-independent, homogeneous functionals and optimise the parameters to best reproduce the k_{xc}^- values for some training set. We used this approach in our recent study⁴¹ of non-interacting kinetic energy functionals (although in that case, the fit was to average, rather than electron deficient, non-interacting kinetic effective homogeneities).

We choose to use a different approach in the present study, which hinges on the fact that we can actually approximate k_{xc}^- for an arbitrary system and so can incorporate it directly into a *system-dependent* functional. Consider the functional

$$E_{xc} = -\frac{J}{N} + \alpha G_{xc}, \quad (12)$$

where we drop the “[ρ]” throughout for notational simplicity. Here, J is the classical Coulomb (Hartree) energy functional, α is a parameter, and

$$G_{xc} = \left[\int \rho^{\frac{3k-m}{3k-m}}(\mathbf{r}) d\mathbf{r} \right]^{\frac{3k-m}{3}}. \quad (13)$$

The first term in Eq. (12) is the Fermi–Amaldi functional,⁴² which is homogeneous of degree 2 under density scaling

and which yields a potential that asymptotically behaves as $-1/r$. The inclusion of this term provides a simple mechanism for introducing the exact asymptotic behaviour into the exchange–correlation potential and has been advocated by Parr and Ghosh.⁴³ Note that we have treated N as a fixed parameter in the functional differentiation in order to obtain an asymptotically vanishing potential; see Refs. 43 and 44 for further discussion. The quantity G_{xc} in Eq. (13) is a local functional of the form considered by Liu and Parr,⁴⁵ which is homogeneous of degree k under density scaling and homogeneous of degree m under coordinate scaling; note the possibility of a non-unity power. Evaluation of Eq. (5) for the functional in Eq. (12) yields effective homogeneities of

$$k_{xc} = \frac{(-2J/N) + k\alpha G_{xc}}{E_{xc}}. \quad (14)$$

Setting k_{xc} equal to k_{xc}^- and rearranging using Eq. (12) then gives

$$k = \frac{k_{xc}^- E_{xc} + (2J/N)}{E_{xc} + (J/N)}. \quad (15)$$

The functional in Eqs. (12) and (13), with the system-dependent k defined in Eq. (15), yields effective homogeneities of k_{xc}^- , as desired, for any α and m .

To turn this into a practical functional, we need to be able to evaluate k for an arbitrary system, which poses an obvious challenge given the form of Eq. (15). However, we observe that all the components on the right hand side of this equation can be estimated from conventional GGA calculations, meaning an approximate k can be calculated in advance and then used in the functional. We do this as follows. The quantities E_{xc} and J are trivially approximated from a GGA calculation; we denote them as E_{xc}^{GGA} and J^{GGA} . For k_{xc}^- , we first rearrange Eq. (9) to give

$$k_{xc}^- = k_{xc}^{av} - \frac{N\Delta_{xc}}{2E_{xc}}, \quad (16)$$

noting from Ref. 38 that $k_{xc}^{av} \approx 4/3$. We also note that Δ_{xc} can be approximated by

$$\Delta_{xc} \approx 2(\epsilon_{\text{HOMO}}^{GGA} + I^{GGA}), \quad (17)$$

where $\epsilon_{\text{HOMO}}^{GGA}$ and I^{GGA} are the HOMO energy and ionisation potential (computed from total electronic energies) determined using a GGA functional. Eq. (17) is central to the asymptotic correction approach of Ref. 46; see Refs. 36 and 47 for further discussion. Substituting these two results into Eq. (16), and estimating E_{xc} using the GGA value, gives

$$k_{xc}^- \approx \frac{4}{3} - \frac{N(\epsilon_{\text{HOMO}}^{GGA} + I^{GGA})}{E_{xc}^{GGA}}. \quad (18)$$

Returning to Eq. (15), we therefore obtain the following expression for the approximate, system-dependent k :

$$k = \frac{\left(\frac{4}{3} - \frac{N(\epsilon_{\text{HOMO}}^{GGA} + I^{GGA})}{E_{xc}^{GGA}}\right) E_{xc}^{GGA} + (2J^{GGA}/N)}{E_{xc}^{GGA} + (J^{GGA}/N)}. \quad (19)$$

The calculation of this quantity requires GGA calculations on the N - and $(N-1)$ -electron systems. The latter is required solely to compute the total electronic energy of the $(N-1)$ -electron system, for the computation of I^{GGA} . The need to

compute the ionisation potential is not only found in the current approach but is also central to conventional global/range separated hybrid tuning approaches involving the HOMO Koopmans condition.

Next, we need to specify values of α and m in Eqs. (12) and (13). In our preliminary investigations, we considered a system-independent α value, obtained from a least-squares fit to a training set using near-exact quantities, for a given m value. However, exchange–correlation energies from the resulting functionals were found to be unsatisfactory, leading us to conclude that system-dependence was also required in α . Given that GGA calculations are already required in advance for the computation of k , it is natural to use these GGA calculations to also compute a system-dependent α . Specifically, we demand that the exchange–correlation energy in Eq. (12) equals the GGA value when the GGA density is used, which requires

$$\alpha = \frac{E_{xc}^{GGA} + (J^{GGA}/N)}{G_{xc}^{GGA}}. \quad (20)$$

Here, G_{xc}^{GGA} is the value of G_{xc} obtained by evaluating Eq. (13) using the GGA density, for the value of k in Eq. (19). This can be obtained from a trivial modification of a GGA code. The only remaining parameter to be specified is m . Test calculations revealed that a value of $m = 1$ led to near-optimal HOMO energies and so we use this value throughout. A value of unity means that G_{xc} is homogeneous of degree one under coordinate scaling and this is not unexpected given that, from Eq. (12), G_{xc} involves the difference between the exchange–correlation and Fermi–Amaldi functionals; both exact exchange (which usually dominates exchange–correlation) and Fermi–Amaldi are homogeneous of degree one under coordinate scaling.

Our scheme for an N -electron system can therefore be summarised as follows: First, we perform GGA calculations on the N - and $(N-1)$ -electron systems and use the data to calculate k using Eq. (19). Next, we determine G_{xc}^{GGA} by evaluating Eq. (13) using the GGA density of the N -electron system, for that calculated value of k , with $m = 1$, and use this quantity in the calculation of α using Eq. (20). Finally, we perform a self-consistent calculation on the N -electron system using the functional in Eqs. (12) and (13) with the calculated values of k and α , and $m = 1$. We denote this functional ED, for “electron deficient.”

We have implemented the ED functional in the CAD-PAC program.⁴⁸ The exchange–correlation potential (for the Kohn–Sham equations) and kernel (for linear-response) were obtained by functionally differentiating both terms in Eq. (12) for constant k , α , m , and N . Special care is required to account for the external power in Eq. (13), particularly for the kernel evaluation. The usual Hellmann–Feynman tests (analytic dipole moment/polarisability vs. finite difference value from energies/dipole moments in an electric field) were used to confirm the validity of our implementation. Note that the parameters defining the ED functional are treated as independent of electric field throughout.

C. Analysis and performance

All ED calculations use the Perdew–Burke–Ernzerhof (PBE) functional⁴⁹ for the initial GGA calculations; we have

confirmed that the results are not sensitive to the choice of GGA. The same basis set is used for each of the three stages of the ED calculations. Given that this is a preliminary, proof-of-concept investigation, we choose not to compare the ED results with those from a plethora of other functionals. We instead focus our comparison against the PBE results, since this is the functional that provides the key ingredients for ED. We also compare with experimental/near-exact reference values, quoting mean absolute errors (MAEs) relative to these values.

We commence by considering results for 8 representative molecules: CH₄, CO, Cl₂, F₂, H₂O, HCl, HF, and N₂, determined at experimental geometries⁵⁰ using the aug-cc-pVTZ basis set. Table I lists the calculated values of k and α from Eqs. (19) and (20), for each molecule, together with the values of $3k/(3k - m)$ and $(3k - m)/3$, which define G_{xc} in Eq. (13). For all 8 systems, the density exponent $3k/(3k - m)$ is greater than unity and so the potential associated with G_{xc} asymptotically vanishes. It follows that the ED exchange–correlation potential in asymptotic regions reduces to the potential of the Fermi-Amaldi functional, which exhibits the exact $-1/r$ form. The ED functional therefore yields the exact asymptotic exchange–correlation potential for each of the 8 systems and we have confirmed that this is the case for all systems considered in this study.

The effective homogeneities of the ED functional are given by Eq. (14) and the central idea behind the functional is that these values should be close to k_{xc}^- . For the 8 molecules, the values of k_{xc}^- were calculated in Ref. 38 and so we can quantify how well this is achieved in practice. Figure 1 compares the ED k_{xc} values, obtained by evaluating Eq. (14) using data from self-consistent calculations with the k and α values in Table I, with the k_{xc}^- values of Ref. 38. The average discrepancy is less than 2% and the system-dependence of k_{xc}^- is successfully reproduced.

Table II presents exchange–correlation energies for the 8 molecules, compared to the near-exact values from Ref. 38. The ED values are very close to those of PBE. The discrepancy between the energies is a measure of the difference between the PBE and ED densities; recall the derivation of Eq. (20). The mean absolute percentage difference between PBE and ED exchange–correlation energies is 0.8%. The discrepancy between total electronic energies (not shown) is just 0.02%.

Table III presents the HOMO energies for the 8 molecules, compared to $-I^0$, the negative of the exact vertical

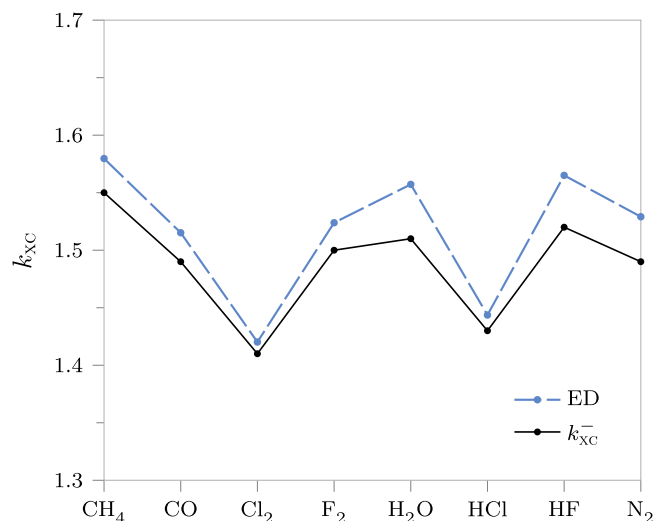


FIG. 1. Comparison of ED effective homogeneities from Eq. (14) with k_{xc}^- values from Ref. 38.

ionisation potential, from Ref. 36. As is well known, the PBE HOMO energies are significantly above $-I^0$, with a MAE of 0.194 a.u. In moving to ED, all HOMO energies are lowered and the MAE reduces to just 0.016 a.u., an order of magnitude improvement.

The importance of the system-dependent, second term in Eq. (12) is illustrated by additional test calculations on the 8 molecules. Removing this term from the functional, leaving only the Fermi-Amaldi term, leads to MAEs in exchange–correlation energies and HOMO energies of 13.007 a.u. and 0.145 a.u., respectively. Reinstating the term, but eliminating its system-dependence by simply using the average values of k and α from Table I, leads to MAEs of 2.501 a.u. and 0.040 a.u. Both sets of errors are significantly larger than the ED errors in Tables II and III.

We now go on to consider the performance of the ED functional for other systems and properties. First, we consider the HOMO energies of bound anions. Most of the molecules in Tables I–III do not vertically bind an excess electron and so we consider a different set. Table IV presents HOMO energies for 11 bound anions, determined at MP2/6-31G* anion geometries using the aug-cc-pVTZ basis set. For reference, we list the negative of the vertical ionisation potential of the anion determined using restricted MP2 (RMP2⁵¹) with the same basis

TABLE I. Parameters defining the ED functional.

Molecule	k^a	α^b	$\frac{3k}{3k-m}$	$\frac{3k-m}{3}$
CH ₄	1.18	-0.590	1.39	0.851
CO	1.19	-0.696	1.39	0.861
Cl ₂	1.22	-0.851	1.37	0.890
F ₂	1.27	-0.643	1.36	0.934
H ₂ O	1.10	-0.639	1.44	0.766
HCl	1.05	-0.913	1.46	0.718
HF	1.09	-0.630	1.44	0.758
N ₂	1.22	-0.661	1.38	0.886

^aFrom Eq. (19).

^bFrom Eq. (20).

TABLE II. Exchange–correlation energies (in a.u.), compared to near-exact values from Ref. 38.

Molecule	PBE	ED	Near-exact
CH ₄	-6.836	-6.922	-6.865
CO	-13.756	-13.835	-13.816
Cl ₂	-56.039	-56.165	-56.303
F ₂	-20.553	-20.665	-20.579
H ₂ O	-9.238	-9.373	-9.270
HCl	-28.377	-28.491	-28.526
HF	-10.713	-10.868	-10.759
N ₂	-13.572	-13.652	-13.607
MAE	0.080	0.074	

TABLE III. HOMO energies (in a.u.), compared to the negative of the exact vertical ionisation potential from Ref. 36.

Molecule	PBE	ED	$-I^0$
CH ₄	-0.347	-0.506	-0.526
CO	-0.332	-0.515	-0.515
Cl ₂	-0.268	-0.414	-0.422
F ₂	-0.347	-0.611	-0.577
H ₂ O	-0.266	-0.466	-0.464
HCl	-0.296	-0.425	-0.469
HF	-0.355	-0.593	-0.592
N ₂	-0.377	-0.593	-0.573
MAE	0.194	0.016	

set. For PBE, the values are essentially all positive and this issue has been the subject of much discussion;^{52,53} the MAE is 0.136 a.u. In moving to ED, all the HOMO values become negative, as required, with a MAE of just 0.016 a.u. (the same as that obtained for the neutral systems in Table III).

Next, we consider TDDFT vertical excitation energies. Table V presents singlet excitation energies for CO, N₂, and H₂CO, determined at experimental geometries⁵⁰ using an augmented Sadlej basis set,^{46,54,55} compared to experimental values.⁴⁶ MAEs are presented for Rydberg, valence, and both categories of excitations combined. Accurate Rydberg excitations require⁴⁶ the exchange–correlation potential to asymptotically behave as $-1/r + \varepsilon_{\text{HOMO}} + I^0$, which reduces to $-1/r$ when Eq. (1) is exactly satisfied. PBE completely fails to exhibit this form and so the Rydberg excitation energies are much too low, as is well known. The ED potential asymptotically behaves as $-1/r$ and approximately satisfies Eq. (1); hence, the potential closely resembles the required form and the Rydberg excitations are significantly improved. The improvement is approximately an order of magnitude for CO and H₂CO, but is less pronounced for N₂, which can be traced to the fact that Eq. (1) is less well satisfied for this system.

For the valence excitations in Table V, the performance of ED is notably less accurate than PBE. A related deficiency is evident in Table VI, which lists static isotropic polarisabilities, determined at experimental geometries⁵⁰ using the Sadlej basis

TABLE IV. HOMO energies (in a.u.), compared to the negative of the RMP2 ionisation potential I .

Anion	PBE	ED	$-I$
CH ₃ S ⁻	0.047	-0.060	-0.070
CN ⁻	-0.001	-0.148	-0.146
Cl ⁻	0.009	-0.103	-0.132
F ⁻	0.057	-0.122	-0.134
HOO ⁻	0.101	-0.069	-0.066
NH ₂ ⁻	0.094	-0.028	-0.033
NO ₂ ⁻	0.040	-0.138	-0.096
OH ⁻	0.080	-0.064	-0.076
PH ₂ ⁻	0.056	-0.028	-0.043
SH ⁻	0.035	-0.061	-0.084
SiH ₃ ⁻	0.034	-0.043	-0.065
MAE	0.136	0.016	

TABLE V. Vertical excitation energies (in eV), compared to experimental values from Ref. 46. Rydberg and valence excitations are labeled R and V, respectively.

State	Transition	Type	PBE	ED	Expt.
CO					
¹ Σ ⁺	$\sigma \rightarrow 3d\sigma$	R	9.62	12.33	12.40
¹ Π	$\sigma \rightarrow 3p\pi$	R	9.56	11.32	11.53
¹ Σ ⁺	$\sigma \rightarrow 3p\sigma$	R	9.47	11.59	11.40
¹ Σ ⁺	$\sigma \rightarrow 3s\sigma$	R	8.99	10.56	10.78
¹ Δ	$\pi \rightarrow \pi^*$	V	10.18	11.11	10.23
¹ Σ ⁻	$\pi \rightarrow \pi^*$	V	9.84	10.39	9.88
¹ Π	$\sigma \rightarrow \pi^*$	V	8.25	8.04	8.51
MAE (R)			2.12	0.17	
MAE (V)			0.12	0.62	
MAE (all)			1.26	0.36	
N₂					
¹ Π _u	$\pi_u \rightarrow 3s\sigma_g$	R	11.54	14.52	13.24
¹ Σ _u ⁺	$\sigma_g \rightarrow 3p\sigma_u$	R	10.47	13.51	12.98
¹ Π _u	$\sigma_g \rightarrow 3p\pi_u$	R	10.48	13.29	12.90
¹ Σ _g ⁺	$\sigma_g \rightarrow 3s\sigma_g$	R	10.23	12.65	12.20
¹ Δ _u	$\pi_u \rightarrow \pi_g$	V	10.08	10.85	10.27
¹ Σ _u ⁻	$\pi_u \rightarrow \pi_g$	V	9.66	9.98	9.92
¹ Π _g	$\sigma_g \rightarrow \pi_g$	V	9.08	9.01	9.31
MAE (R)			2.15	0.66	
MAE (V)			0.23	0.32	
MAE (all)			1.33	0.51	
H₂CO					
¹ A ₂	$n \rightarrow 3db_1$	R	7.14	9.64	9.22
¹ A ₂	$n \rightarrow 3pb_1$	R	6.59	8.46	8.38
¹ B ₁	$\sigma \rightarrow \pi^*$	V	8.85	8.94	8.68
¹ B ₂	$n \rightarrow 3pa_1$	R	6.38	8.04	8.12
¹ A ₁	$n \rightarrow 3pb_2$	R	6.40	8.25	7.97
¹ B ₂	$n \rightarrow 3sa_1$	R	5.73	7.24	7.09
¹ A ₂	$n \rightarrow \pi^*$	V	3.80	3.48	3.94
MAE (R)			1.71	0.20	
MAE (V)			0.16	0.36	
MAE (all)			1.26	0.25	

set, compared to reference BD(T) values determined using the same basis set.⁵⁶ The PBE values are too high. ED does reduce the values, but by significantly too much.

Finally, Figure 2 plots the exchange–correlation potentials along the bond axis of two representative systems, CO and PN, compared to the near-exact $v_{\text{xc}}^-(\mathbf{r})$ of Ref. 57, determined using the procedure of Zhao, Morrison, and Parr (ZMP).³⁹ The present calculations use the same Huzinaga basis set as was used in Ref. 57. The PBE potentials are well above the near-exact potentials and do not exhibit a $-1/r$ asymptotic behaviour; they rapidly decay to zero with increasing distance from the molecule. In moving to ED, the potentials lower towards the near-exact potential (and it is this lowering in energetically important regions that causes $\varepsilon_{\text{HOMO}}$ to reduce towards $-I^0$) and the exact $-1/r$ behaviour is attained. There is, however, clear room for improvement in non-asymptotic regions. In particular, the ED potentials do not exhibit the intershell structure evident in both PBE and the near-exact potential and this is a consequence of the fact that G_{xc} is a local, rather than gradient corrected, functional.

TABLE VI. Static isotropic polarisabilities (in a.u.), compared to reference BD(T) values from Ref. 56.

Molecule	PBE	ED	BD(T)
C ₂ H ₄	28.30	24.97	26.91
CH ₄	17.40	15.79	16.43
Cl ₂	31.54	28.70	30.71
CO	13.53	11.73	13.03
CO ₂	17.72	15.72	17.56
F ₂	8.87	7.68	8.45
H ₂ O	10.49	8.53	9.71
H ₂ S	25.70	24.18	24.67
HCl	18.26	16.64	17.43
HF	6.18	4.86	5.64
N ₂	12.13	10.28	11.75
NH ₃	15.37	12.96	14.33
PH ₃	31.85	31.57	30.44
SO ₂	26.44	24.26	26.06
MAE	0.76	1.25	

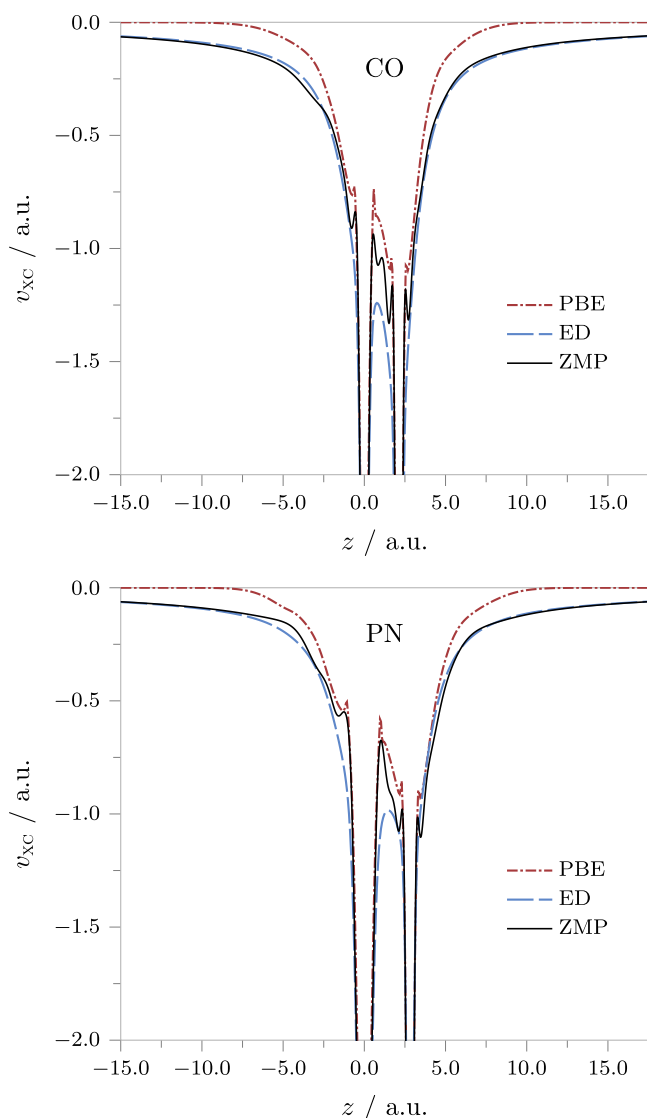


FIG. 2. Exchange–correlation potentials along the bond axis for CO and PN, compared to the near-exact ZMP potential from Ref. 57.

We have therefore achieved our aim. Our method does yield a functional that is appropriate for the electron deficient side of the integer, as illustrated by the effective homogeneities in Figure 1, the HOMO energies in Tables III and IV, and the exchange–correlation potentials in Figure 2. The ability to recover the exact asymptotic potential is an added bonus, yielding the improved Rydberg excitations in Table V. The functional is less successful for the valence excitations in Table V and static isotropic polarisabilities in Table VI, which is consistent with the lack of quantitative accuracy in the shape of the exchange–correlation potentials in non-asymptotic regions (Figure 2). We should not be surprised by deficiencies. The functional form is extremely simple, with a purely local G_{xc} term. It is also instructive to consider precisely what our functional development procedure imposes. We constrain k_{xc} to be close to k_{xc}^- and E_{xc} to be close to the (reasonably accurate) GGA value. It therefore follows from Eqs. (5) and (7) that the ED functional must yield a reasonably accurate $\int v_{xc}(\mathbf{r})\rho(\mathbf{r})d\mathbf{r}$. This is clearly desirable, but is not a sufficient condition to ensure that the potential itself has the correct shape (consistent with our observations for Figure 2). An additional factor that may affect the accuracy of excited states and polarisabilities is the neglect of electric field dependence of the functional parameters.

Looking ahead, an obvious next step is to introduce gradient dependence into G_{xc} , although particular care will be required to avoid divergence of the potential in asymptotic or zero density gradient regions. One might also be tempted to use ED data to calculate new k and α values and then iterate the approach. We emphasise that Eq. (19) relies on the use of a GGA HOMO energy; if the ED HOMO energy is instead used, then the overall effective homogeneity will be close to 4/3 for all systems. It is also important to note that the ED functional form is not size-extensive. Regarding the shape of the potential, it may prove fruitful to explicitly enforce the correct shape in the spirit of Ref. 56. Finally, the dependence of the parameters k and α on perturbations, such as electric fields and nuclear coordinates, must be investigated. Again, this latter issue is not only found in the current approach but also arises in conventional global/range separated hybrid tuning approaches, where the tuning parameter has a perturbation dependence.²⁹ Investigations are underway.

III. CONCLUSIONS

We have used density scaling considerations to derive an exchange–correlation explicit density functional that is appropriate for the electron deficient side of the integer and which recovers the exact $r \rightarrow \infty$ asymptotic behaviour of the exchange–correlation potential. The functional has an unconventional mathematical form with parameters that are system-dependent; the parameters for an N -electron system are determined in advance from GGA calculations on the N - and $(N - 1)$ -electron systems. Compared to GGA results, the functional yields similar exchange–correlation energies, but HOMO energies that are an order of magnitude closer to the negative of the vertical ionisation potential; for anions, the HOMO energies are negative, as required. Rydberg excitation energies are also notably improved and the

exchange–correlation potential is visibly lowered towards the near-exact potential. Further development is required to improve valence excitations, static isotropic polarisabilities, and the shape of the potential in non-asymptotic regions.

The ED functional is fundamentally different to conventional approximations. We hope that the ideas used in its derivation and the insight they provide may prove useful in future functional development studies.

ACKNOWLEDGMENTS

The authors are grateful to Alex Borgoo, James A. Green, and Michael J. G. Peach for helpful discussions. We thank the EPSRC for studentship support.

- ¹J. P. Perdew, R. G. Parr, M. Levy, and J. L. Balduz, *Phys. Rev. Lett.* **49**, 1691 (1982).
- ²W. Kohn and L. J. Sham, *Phys. Rev.* **140**, A1133 (1965).
- ³P. Mori-Sánchez, A. J. Cohen, and W. Yang, *J. Chem. Phys.* **125**, 201102 (2006).
- ⁴A. Ruzsinszky, J. P. Perdew, G. I. Csonka, O. A. Vydrov, and G. E. Scuseria, *J. Chem. Phys.* **126**, 104102 (2007).
- ⁵A. J. Cohen, P. Mori-Sánchez, and W. Yang, *Science* **321**, 792 (2008).
- ⁶R. Haunschild, T. M. Henderson, C. A. Jiménez-Hoyos, and G. E. Scuseria, *J. Chem. Phys.* **133**, 134116 (2010).
- ⁷O. A. Vydrov, G. E. Scuseria, and J. P. Perdew, *J. Chem. Phys.* **126**, 154109 (2007).
- ⁸A. Ruzsinszky, J. P. Perdew, G. I. Csonka, O. A. Vydrov, and G. E. Scuseria, *J. Chem. Phys.* **125**, 194112 (2006).
- ⁹A. J. Cohen, P. Mori-Sánchez, and W. Yang, *J. Chem. Phys.* **126**, 191109 (2007).
- ¹⁰A. D. Dutoi and M. Head-Gordon, *Chem. Phys. Lett.* **422**, 230 (2006).
- ¹¹Y. Zhang and W. Yang, *J. Chem. Phys.* **109**, 2604 (1998).
- ¹²B. G. Johnson, C. A. Gonzales, P. M. Gill, and J. A. Pople, *Chem. Phys. Lett.* **221**, 100 (1994).
- ¹³A. J. Cohen, P. Mori-Sánchez, and W. Yang, *Phys. Rev. B* **77**, 115123 (2008).
- ¹⁴T. Bally and G. N. Sastry, *J. Phys. Chem. A* **101**, 7923 (1997).
- ¹⁵Y. Xie, H. F. Schaefer, X.-Y. Fu, and R.-Z. Liu, *J. Chem. Phys.* **111**, 2532 (1999).
- ¹⁶D. J. Tozer, *J. Chem. Phys.* **119**, 12697 (2003).
- ¹⁷A. Seidl, A. Görling, P. Vogl, J. Majewski, and M. Levy, *Phys. Rev. B* **53**, 3764 (1996).
- ¹⁸R. Rios-Font, M. Sodupe, L. Rodríguez-Santiago, and P. R. Taylor, *J. Phys. Chem. A* **114**, 10857 (2010).
- ¹⁹O. A. Vydrov and G. E. Scuseria, *J. Chem. Phys.* **125**, 234109 (2006).
- ²⁰E. Dumont, A. D. Laurent, X. Assfeld, and D. Jacquemin, *Chem. Phys. Lett.* **501**, 245 (2011).
- ²¹U. Salzner and R. Baer, *J. Chem. Phys.* **131**, 231101 (2009).
- ²²T. Stein, H. Eisenberg, L. Kronik, and R. Baer, *Phys. Rev. Lett.* **105**, 266802 (2010).
- ²³T. Stein, L. Kronik, and R. Baer, *J. Am. Chem. Soc.* **131**, 2818 (2009).
- ²⁴T. Stein, L. Kronik, and R. Baer, *J. Chem. Phys.* **131**, 244119 (2009).
- ²⁵N. Kuritz, T. Stein, R. Baer, and L. Kronik, *J. Chem. Theory Comput.* **7**, 2408 (2011).
- ²⁶S. Refaely-Abramson, R. Baer, and L. Kronik, *Phys. Rev. B* **84**, 075144 (2011).
- ²⁷T. Minami, M. Nakano, and F. Castet, *J. Phys. Chem. Lett.* **2**, 1725 (2011).
- ²⁸L. Kronik, T. Stein, S. Refaely-Abramson, and R. Baer, *J. Chem. Theory Comput.* **8**, 1515 (2012).
- ²⁹A. Karolewski, L. Kronik, and S. Kümmel, *J. Chem. Phys.* **138**, 204115 (2013).
- ³⁰J. D. Gledhill, M. J. G. Peach, and D. J. Tozer, *J. Chem. Theory Comput.* **9**, 4414 (2013).
- ³¹A. Karolewski, T. Stein, R. Baer, and S. Kümmel, *J. Chem. Phys.* **134**, 151101 (2011).
- ³²T. Körzdörfer, R. M. Parrish, J. S. Sears, C. D. Sherrill, and J.-L. Brédas, *J. Chem. Phys.* **137**, 124305 (2012).
- ³³H. Sun and J. Autschbach, *ChemPhysChem* **14**, 2450 (2013).
- ³⁴P. Agrawal, A. Tkatchenko, and L. Kronik, *J. Chem. Theory Comput.* **9**, 3473 (2013).
- ³⁵A. J. Garza, O. I. Osman, A. M. Asiri, and G. E. Scuseria, *J. Phys. Chem. B* **119**, 1202 (2015).
- ³⁶A. M. Teale, F. De Proft, and D. J. Tozer, *J. Chem. Phys.* **129**, 044110 (2008).
- ³⁷S. Liu and R. G. Parr, *Phys. Rev. A* **53**, 2211 (1996).
- ³⁸A. Borgoo, A. M. Teale, and D. J. Tozer, *J. Chem. Phys.* **136**, 034101 (2012).
- ³⁹Q. Zhao, R. C. Morrison, and R. G. Parr, *Phys. Rev. A* **50**, 2138 (1994).
- ⁴⁰M. Levy and J. P. Perdew, *Phys. Rev. A* **32**, 2010 (1985).
- ⁴¹A. Borgoo, J. A. Green, and D. J. Tozer, *J. Chem. Theory Comput.* **10**, 5338 (2014).
- ⁴²E. Fermi and E. Amaldi, *Accad. Ital. Rome* **6**, 117 (1934).
- ⁴³R. G. Parr and S. K. Ghosh, *Phys. Rev. A* **51**, 3564 (1995).
- ⁴⁴D. J. Tozer, *Phys. Rev. A* **56**, 2726 (1997).
- ⁴⁵S. Liu and R. G. Parr, *Phys. Rev. A* **55**, 1792 (1997).
- ⁴⁶D. J. Tozer and N. C. Handy, *J. Chem. Phys.* **109**, 10180 (1998).
- ⁴⁷S. R. Whittleton, X. A. Sosa Vazquez, C. M. Isborn, and E. R. Johnson, *J. Chem. Phys.* **142**, 184106 (2015).
- ⁴⁸R. D. Amos, I. L. Alberts, J. S. Andrews, A. J. Cohen, S. M. Colwell, N. C. Handy, D. Jayatilaka, P. J. Knowles, R. Kobayashi, G. J. Laming, A. M. Lee, P. E. Maslen, C. W. Murray, P. Palmieri, J. E. Rice, E. D. Simandiras, A. J. Stone, M.-D. Su, and D. J. Tozer, CADPAC 6.5, The Cambridge Analytic Derivatives Package, Cambridge, UK, 1998.
- ⁴⁹J. P. Perdew, K. Burke, and M. Ernzerhof, *Phys. Rev. Lett.* **77**, 3865 (1996).
- ⁵⁰N. C. Handy and D. J. Tozer, *Mol. Phys.* **94**, 707 (1998).
- ⁵¹D. J. Tozer, N. C. Handy, R. D. Amos, J. A. Pople, R. H. Nobes, Y. Xie, and H. F. Schaefer, *Mol. Phys.* **79**, 777 (1993).
- ⁵²J. M. Galbraith and H. F. Schaefer III, *J. Chem. Phys.* **105**, 862 (1996).
- ⁵³N. Rösch and S. B. Trickey, *J. Chem. Phys.* **106**, 8940 (1997).
- ⁵⁴A. J. Sadlej, *Theor. Chim. Acta* **79**, 123 (1991).
- ⁵⁵A. J. Sadlej, *Collect. Czech. Chem. Commun.* **53**, 1995 (1988).
- ⁵⁶P. J. Wilson, T. J. Bradley, and D. J. Tozer, *J. Chem. Phys.* **115**, 9233 (2001).
- ⁵⁷T. W. Keal and D. J. Tozer, *J. Chem. Phys.* **119**, 3015 (2003).